RESEARCH ARTICLE | OCTOBER 06 2023

Static optimal control: A closed-loop control strategy for heliostat aiming in solar power towers

David Zanger ✉; Laurin Oberkirsch; Daniel Maldonado Quinto; Robert Pitz-Paal

AIP Conf. Proc. 2815, 030022 (2023)
https://doi.org/10.1063/5.0149422

Static Optimal Control: A Closed-Loop Control Strategy for Heliostat Aiming in Solar Power Towers

David Zanger[a)], Laurin Oberkirsch, Daniel Maldonado Quinto and Robert Pitz-Paal

Institute of Solar Research, German Aerospace Center (DLR), Linder Hoehe, 51147 Cologne (Germany)

[a)] Corresponding author: david.zanger@dlr.de

Abstract. In this paper, a new closed-loop control for the heliostat aiming of solar tower power plants is proposed. It is called Static Optimal Control and is based upon the ant-colony optimization meta-heuristic. The controller can increase the plant's efficiency, restrict the flux density and compensate for disturbances such as clouds. It is tested on small reference plant with a test case considering a suddenly appearing cloud disturbance. Within the test case, the controller could compensate for a mirror error which caused a drop of the relative power of around 3%. During the cloudy phase, the controller increased the relative power by 1%. The overflux condition which occurred after the cloud suddenly disappeared could be eliminated within 12 control steps. However, this number can be reduced by adjusting the controller parameters.

INTRODUCTION

To make solar tower power plants more economical, an increase in the plant's efficiency is important. One possibility to increase the efficiency is by optimizing the irradiance distribution over the receiver module. The objective is to minimize spillage, while the irradiance must be limited to prevent damage to the receiver. Furthermore, the solar tower power plant is subject to disturbances such as clouds. Due to dynamic changes in the sun's position and the limit of the irradiance during operation as well as the disturbances, an open- or closed-loop controller is required, which can react to these changes. In literature, there exist predominantly open-loop controllers, which try to find aim point configurations yielding a near optimal flux density distribution on the receiver. Many of these controllers solve an NP-hard combinatorial optimization problem by using for example an ant-colony optimization meta-heuristic [1], the TABU algorithm [2] or a MILP solver [3]. Most of these optimizers can only solve for problems with a small heliostat field in an adequate time. However, commercial plants usually consist of several thousands of heliostats. Here, the ant-colony optimization meta-heuristic [14] or the MILP based approach HALOS [15] may be appropriate. Other control algorithms, use heuristic techniques exist such as the Static Aimpoint Processing System (SAPS) algorithm by Vant-Hull, which was modified by Flesch et al [4]. However, all these open-loop controllers lack the possibility to compensate for modeling errors like an inaccurate estimation of the mirror and tracking error or disturbances such as clouds.

A closed-loop controller can overcome these problems. In literature, there exist some heuristic closed-loop controllers such as Dynamic Aimpoint Processing System (DAPS) by Vant-Hull [5], which can only compensate for overflux conditions or more complex ones like PID [6] or MPC [7] controllers. However, none can maximize the power on the receiver while rejecting disturbances based on flux density measurements for different receiver shapes. This paper introduces a new control approach based on the ant colony optimization, which can fulfill these requirements. The control approach shall increase the optical efficiency of the solar tower power plant by increasing the power on the receiver. However, damage from the receiver shall be prevented and therefore, the maximum flux density must be restricted. Furthermore, the controller shall compensate for modeling errors such as inaccurate modelled tracking or mirror errors as well as dynamic disturbances such as clouds. Additionally, the controller should be able to work with different receiver types (e.g. cylindrical or rectangular receivers).

SolarPACES: Solar Power & Chemical Energy Systems
AIP Conf. Proc. 2815, 030022-1–030022-8; https://doi.org/10.1063/5.0149422
Published by AIP Publishing. 978-0-7354-4623-6/$30.00

The development of a control strategy fulfilling these requirements follows the process of control system design as stated by Skogestad and Postlethwaite [8]. Thus, the system plant is analyzed at first and some general properties of the controller are determined. Subsequently, a new control approach called the Static Optimal Control is developed and explained in detail. Afterwards, the controller is tested in a simulation case and the results are presented. Finally, conclusion and outlook are given.

SYSTEM AND CONTROLLER PROPERTIES

Plant System

In a solar tower power plant, a multitude of heliostats reflect the solar radiation onto a receiver. For every heliostat, an aim point on the receiver can be chosen. A specific aim point configuration then results in a flux density distribution on the receiver, which can be measured. Thus, the system belongs to the class of multiple-input multiple-output (MIMO) systems, with aim points as inputs and a flux density distribution as output. A solar power tower plant usually represents a large MIMO-system. For example, the Solar Two tower has 1926 heliostats with in total 3852 inputs considering two aim point coordinates per heliostat. And it measures a flux density image of the size 24x21 resulting in 504 outputs. Secondly, the plant system is a non-linear system. This can be concluded for example by considering the HFLCAL model, which is based on a bivariate normal distribution [9]. The model describes the flux density F at one point (x, y) on the receiver for a heliostat h aiming at a specific aim point (x_a, y_a) according to Equation 1.

$$F_{x,y}^{(h)} = \frac{P_H \cos \omega_p}{2\pi\sigma_{HF}^2} e^{-\frac{(x-x_a)^2+(y-y_a)^2}{2\pi\sigma_{HF}^2}} \tag{1}$$

In the equation, P_H denotes the power reflected by the heliostat, σ_{HF} is the total effective deviation and ω_p represents the angle between the normal vector of the receiver and the heliostat. As it can be seen, the flux density depends on the aim point in a non-linear way. The function could be linearized for a given aim point to remove the non-linearity. However, this is not reasonable as the aim point usually shifts in larger quantities, which invalidates the linear model.

Furthermore, the system is stable in the sense that a bounded input yields a bounded output of the system. The system is bounded by the maximum possible flux density. This upper bound is reached when all aim points target the center of the receiver

A crucial assumption is that the system without the influence of disturbances can be considered static. This assumption is only valid, when the sample time is higher than the time the heliostats need to move from one aim point to another. Furthermore, this assumes a static sun, which is valid as long as only a small time interval (around 5 min) is considered. The controller's objective is to reject modeling errors and disturbances. The wrong sun position can be seen as a modeling error. Thus, the assumption is reasonable in this case. Furthermore, in this paper, only small time intervals are considered in which the sun position does not change significantly.

All in all, the controller needs to control a plant, which has the properties of a non-linear, stable and static MIMO system. This is untypical for plant systems in control theory, in which stabilizing a dynamic plant system is usually the main objective of the controller.

Controller In- and Outputs

Before designing a specific controller, the in- and outputs of the controller must be determined. In literature, the common choice for the inputs are the aim point coordinates, which is adopted in this work. The flux density distribution is chosen as output because the control of this variable has a direct influence on the intercepted power of the receiver and thus, the efficiency of the plant, which coincides with the objective of the thesis. The flux density can for example be measured by a camera supported sensor [10]. Furthermore, by choosing the flux density distribution as output, the simulation is simplified by not needing to model the thermal side. This would be the case when setting the temperature distribution as output.

STATIC OPTIMAL CONTROL

To control the plant system, a controller, which is capable to control a static non-linear multi-input multi-output (MIMO) system, has to be designed. Within literature, most control algorithms are designed for linear dynamic systems. Therefore, a novel control approach is developed to control the non-linear static system. The idea is to adapt an existing open-loop controller for solar power tower plants to a closed-loop controller by integrating a feedback. In this work, an open-loop control using an optimization algorithm is extended. The idea is that the new controller would inherit the advantages of the optimization algorithm, which is the general formulation with respect to the receiver type and the disturbances. This new approach is referred to as Static Optimal Control.

The controller maximizes an optimization problem, which is defined in equation 2.

$$\max_{\mathbf{u}} J\,(\hat{\boldsymbol{y}}, \boldsymbol{w}) \qquad s.t.\ \hat{\boldsymbol{y}} \leq \boldsymbol{y_{max}} \tag{2}$$

Here, J denotes the objective function, $\hat{\boldsymbol{y}}$ is the flux density distribution calculated by a simulation given the aim point configuration $\boldsymbol{u}$. Furthermore, $\boldsymbol{y_{max}}$ represents the allowed flux density and $\boldsymbol{w}$ the weights. All vectors have a size of n_{bins} except for $\boldsymbol{u}$, whose length is equal to the number of aim points $n_{\text{aimpoints}}$. n_{bins} denotes the number of measurement points e.g. pixel of a camera. In every control step, the weights of the objective function are calculated based on the measured error $\boldsymbol{e}$. The weights are estimated by a weight calculator so that the optimization algorithm yields a solution, which reduces the error.

The controller can be divided into the following functional components: The optimization algorithm (including the objective function), the error signal calculator and the weight calculator, which are shown in Fig. 1. These components are explained in more detail in the next paragraphs.

Optimization Algorithm

The optimization algorithm solves the stated problem mentioned in the previous paragraph. As optimizer, the ant colony optimization is chosen, which was adapted for the heliostat aiming problem by Belhomme [11]. The algorithm showed to find near optimal solutions in an adequate time. In addition, the implementation of the algorithm is property of the DLR and thus, the source code was open to the author. The optimization algorithm uses the solar tower raytracing laboratory (STRAL) introduced by Belhomme [11] to calculate the flux density distribution. STRAL is a Monte Carlo raytracing tool, which can simulate the flux density distribution with a very high accuracy in a small amount of time [12]. The model is implemented in C++ due to the high computational effort of the optimizer.

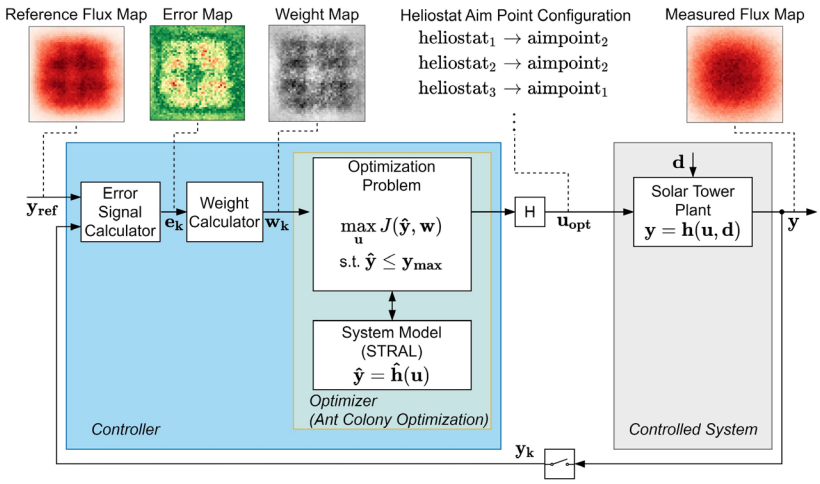

FIGURE 1. Static Optimal Control scheme. Above every signal, a sample signal is depicted.

Objective Function

The objective function of the optimization algorithm depends on the simulated flux density distribution $\hat{\mathbf{y}}$, the allowed flux density $\mathbf{y_{max}}$ and the weights $\mathbf{w}$, which are estimated by the weight calculator. Other variables are also possible, such as the covered distance of the aim point shift to restrict the heliostat movement. However, this is not within the scope of this work. Within this work the objective function presented in equation 3 is used.

$$J = \mathbf{w}^{\mathrm{T}}\hat{\mathbf{y}} - \mathrm{p}\sum_i max\left(\hat{\boldsymbol{y}}_i - \boldsymbol{y}_{i,\max}, 0\right) \tag{3}$$

The objective value increases with an increasing simulated flux density, which is dependent on the chosen aim points. A high overall simulated flux density is desired, because it increases the efficiency of the plant. However, if the simulated flux density exceeds the allowed flux density, the objective value is reduced by the overflux multiplied with the penalty factor. This additional term is a soft constraint to restrict the maximum flux density. Because it is a soft constraint, slight violations of the constraints are still valid. The objective of the weights is to direct the heliostats to aim points to correct uncertainties or inaccuracies in the simulation like unknown disturbances or modeling errors.

Due to the formulation of the ant colony algorithm, the objective value is not allowed to be less or equal than zero and should be in the magnitude of one. Thus, the objective value has to be scaled, due to the fact that the proposed objective function can yield negative values or values greater than one. Within this work a simple linear scaling function is used.

Error Signal

The error is fed to the weight calculator. To calculate the error from the measured flux density distribution y and the reference flux density distribution $\boldsymbol{y}_{ref}$, a formulation according equation 4 is proposed.

$$\boldsymbol{e} = \frac{\boldsymbol{y_{ref}} - \boldsymbol{y}}{|\boldsymbol{y_{ref}}|_\infty} \tag{4}$$

In this formulation, the error is scaled by the maximum flux density of the reference signal. Therefore, the error is around one and thus, the magnitude of the weights is more determined by the parameters of the weight calculator than by the error signal. Additionally, this allows to change the reference flux density distributions without changing the parameters of the weight calculator.

Weight Calculator

The weight calculator calculates the weights used in the objective function and thus, makes the optimization algorithm concentrate the radiation more on certain bins than on others. In general, the weight calculator increases the weights, when the error is positive, i.e., when the measured flux density is lower than the reference flux density. Since the algorithm tends to focus on bins with high weights, the increased weights reduce the error. When the error is negative, the weight calculator decreases the weights to defocus the heliostats at that point and thus, reduces the error. The weight calculator presented in equation 5 is used in this work.

$$\boldsymbol{w}_{k+1} = \boldsymbol{w}_k + K_{\mathrm{i}} \cdot \boldsymbol{e}_k \tag{5}$$

The weight calculator resembles an integrator, which increases the current weight by the current error multiplied with the factor K_i. An integrator in control theory has the advantage that it does not permit a permanent control deviation, but it has the disadvantage that it reacts rather slow [13].

RESULTS

Test Case

The simulated plant is a small plant with a rectangular receiver and 100 heliostats arranged in a north-field layout as shown in Fig. 2. The field is very small compared to commercial plants with thousands of heliostats. This was done due to the computational effort of the simulation (1.14 s per control step), especially when running parameter studies to tune the controller. For a first test this seems still reasonable as usually for large plants the heliostats are grouped into a few hundred groups.

Relevant parameters for receiver, heliostats and environment are stated in Table 1. For simplicity, this test case considers a homogenous allowed flux density distribution of 50 kW/m². However, an inhomogeneous distribution can also be used for the optimizer and was already tested in [16]. The allowable flux density is significantly lower than the maximum possible flux density and thus, forces the controller to find a solution, which differs from the trivial solution of pointing all heliostats at the center. The aim points are distributed on a 5x5 grid and the measurement points on a 50x50 grid as illustrated in Fig. 2. Optical losses such as cosine loss, mirror reflectivity and air attenuation are considered.

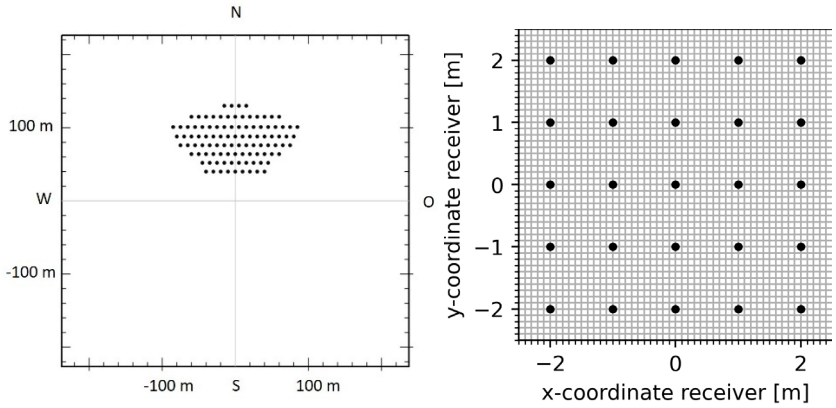

FIGURE 2. Field layout of the small reference plant (left) and aim point coordinates and measurement grid (right).

TABLE 1. Parameters of the solar power tower plant.

Parameters Ambient and Tower	Value	Parameters Heliostat	Value
Latitude location	37.095°	Total reflective area	8 m²
Longitude location	-2.36°	Facets vertical direction	2
Ambient temperature	298.15 K	Facets horizonal direction	2
Metres above sea level	500 m	Facet width	1.25 m
DNI	850 W/m²	Facet height	1.6 m
CSR sun distribution	5	Gaps between facets	None
Azimuth sun position	0°	Pedestal height	2 m
Elevation sun position	45°	Focal length	0 m
Tower height to receiver center	60 m	Canting point	0, 0, 100m
Height	5 m	Tracking error	0 mrad
Width	5 m	Total reflectivity	0.92
Measurement bins horizontal	50	Axis offset	0 m
Measurement bins vertical	50		

Within this work, a test case, which includes three common cases is tested to examine the control quality of the controller. At step 0, the mirror error of the heliostats is increased from 0 to 3 mrad. Then, the controller has 30 control steps to compensate for the error. After 30 steps, a cloud is simulated by setting the DNI to zero for half the heliostats. This is equivalent to the case that clouds shade half of the field. After another 30 control steps, at step 60, the clouds pass i.e. the DNI is set to the initial intensity again.

The presented test case covers most of the situations the controller will face in a real application. On the one hand, the mirror error decreases and widens the flux density distribution. In reality, other optical errors have a similar influence. They usually reduce and/or broaden the flux density distribution. Therefore, simulating the mirror error is a good choice to represent different optical losses. On the other hand, shading half of the field simulates a large deviation. This tests the controller's ability to operate with high modeling errors as well as dynamic disturbances. In addition, a disappearing cloud can lead to overflux conditions. Therefore, this test case additionally tests the response to an overflux condition.

Controller Parameters

The number of runs and ants are set to 50 for the ant colony optimization. β, the pheromone start value, ρ, and q_0 of the optimization are set to 2, 0.01, 0.15 and 0.98 respectively (see [1] for an explanation of these parameters). The number of control steps is set to 100 because the algorithm usually converges during this number of steps. The weights are always initialized with 1. The reference flux density distribution is pictured in Fig. 1. It was determined using the ant colony optimization algorithm to find an optimal aim point configuration considering the allowable flux density of 50 kW/m² without a mirror error. For the evaluation the penalty p and the parameter K_i are varied.

Evaluation Criteria

The relative power is defined by the ratio of the current power to the assumed maximal power, which was estimated through an optimization. The error of the relative power is defined as the difference of the current relative power and the relative power of one. The mean of the last twenty steps μ_{l20} is considered to determine the degree to which the mirror can be compensated for.

For the evaluation of the clouds two additional criteria are considered. The first criterion k_{noc} (noc = no overflux condition) states how many control steps the controller needs to eliminate the overflux condition, which may arise after the clouds pass. This may happen due to the fact that the heliostats are usually centered during the cloudy phase. Then, when the full radiation is available after the clouds disappear, too many heliostats may be centered, which leads to an overflux condition.

The second criterion describes the final convergence value of the relative power during the cloud phase. This criterion is expressed by the mean relative power μ_{cloud} of step 49 to 59, the final phase before the cloud passes at step 60. A low value for k_{noc} and high value for μ_{cloud} are desired. However, a higher μ_{cloud} value usually leads to a higher overflux after the clouds passes because the controller concentrated the flux more in the center. To eliminate a higher overflux, the controller usually needs more steps. Thus, a higher μ_{cloud} usually leads to a higher k_{noc}.

Each parameter combination is run five times and the results are averaged to account for fluctuations of the non-deterministic ant colony optimization.

Evaluation

Most parameter combinations caused an overflux condition after the cloud passed. There are also parameter combinations, which did not cause an overflux condition after the cloud passed. However, these combinations usually performed worse with respect to the μ_{cloud} and μ_{l20} value. In Table 2 the best values for the criteria k_{noc}, μ_{cloud} and μ_{l20} for a given parameter combination are stated. In all cases, the applied mirror error, which resulted in an initial relative power of 95.84%, is almost compensated completely (see μ_{l20} value). Depending on the dominating criteria, the μ_{cloud} value deviates by 0.81 percentage points. The biggest deviation can be noticed regarding the k_{noc} value. Here, zero is probably most desirable to safely exclude damage to the receiver. However, depending on the sample time and the receiver state and characteristic, values higher than zero might be acceptable.

TABLE 2. Averaged results from the test case (average of five runs).

k_{noc}	μ_{cloud}	μ_{l20}	p	K_i
0	49.72%	99.17%	100	5
14	50.53%	99.34%	100	100
12	50.47%	99.36%	10	5

An overview of the control trajectory and the overflux for the control configuration with the highest μ_{l20} value is shown in Fig. 3. Here the controller compensates the mirror error and increases the relative power by 3.06 percentage points to 98.92% in step 29. Then, the cloud appears and the relative power drops to 49.47%. The controller compensates for the clouds and increases the relative power by around 1% to a value of 50.42%. However, this is still 2.57% away from the maximum of 52.99%. When the cloud disappears abruptly, it arises an overflux condition, which is erased after 13 steps.

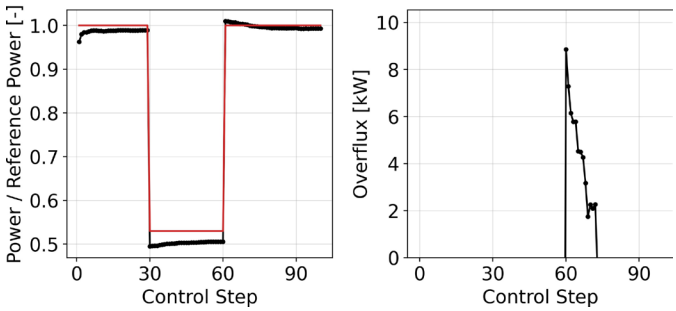

FIGURE 3. Results of the test case. The black line depicts the output from the simulation model and the red line the assumed optimum considering the limit given by the allowed flux density.

CONCLUSION AND OUTLOOK

In this work, a novel closed-loop control strategy for heliostat aiming of solar power tower plants was presented. The approach, which is called Static Optimal Control, modifies the existing ant colony optimization algorithm for heliostat aiming to work as a closed-loop control. Overall, the developed controller could fulfill the objectives of this work, namely increasing the optical efficiency, restricting the flux density and compensating for disturbances such as clouds. However, the controller does not completely compensate for clouds. Here, improvements could be made, such as adapting the objective function or the weight estimator. Further investigation considering greater number of heliostats and aim points, different receiver types, inhomogeneous and varying allowable flux density distributions as well as tests on the solar tower in Jülich will be published in the near future.

ACKNOWLEDGMENTS

This work was carried out in the project “HeliBo” (Grant No.: PRO0070 A) with the financial support from the Ministry of Economic Affairs, Innovation, Digitalization and Energy of the State of North Rhine-Westphalia.

REFERENCES

1. B. Belhomme, R. Pitz-Paal, and P. Schwarzbözl, *Journal of Solar Energy Engineering*, no. 1, 2014.
2. A. Salomé, F. Chhel, G. Flamant, A. Ferrière, and F. Thiery, *Solar Energy*, pp. 352–366, 2013.
3. T. Ashley, E. Carrizosa, and E. Fernández-Cara, *Energy*, pp. 285–291, 2017.
4. R. Flesch, C. Frantz, D. Maldonado Quinto, and P. Schwarzbözl, *Solar Energy*, pp. 1273–1281, 2017.
5. L. L. Vant-Hull, *Journal of Solar Energy Engineering*, no. 2, pp. 165–169, 2002.

6. J. García, Y. C. Soo Too, R. Vasquez Padilla, R. Barraza Vicencio, A. Beath, and M. Sanjuan, “Heat Flux Distribution Over a Solar Central Receiver Using an Aiming Strategy Based on a Conventional Closed Control Loop,” in *2017 proceedings of the ASME 11th International Conference on Energy Sustainability/15th Fuel Cell Science, Engineering, and Technology Conference*, 2017.
7. J. García, Y. Chean Soo Too, R. Vasquez Padilla, A. Beath, J.-S. Kim, and M. E. Sanjuan, *Journal of Solar Energy Engineering*, 2018.
8. S. Skogestad and I. Postlethwaite, *Multivariable feedback control: Analysis and design,* 2nd ed. Chichester: Wiley, 2009.
9. M. Kiera, “Heliostat Field: Computer Codes, Requirements, Comparison of Methods,” 1989.
10. M .Offergeld, M. Röger, H. Stadler, P. Gorzalka, and B. Hoffschmidt, "Flux density measurement for industrial-scale solar power towers using the reflection off the absorber", *AIP Conference Proceedings 2126*, 2019, 110002, https://aip.scitation.org/doi/abs/10.1063/1.5117617.
11. B. Belhomme, “*Bewertung und Optimierung von Zielpunktstrategien für solare Turmkraftwerke*, ”Ph.D. thesis. RWTH Aachen, 2011.
12. B. Belhomme, R. Pitz-Paal, P. Schwarzbözl, and S. Ulmer, *Journal of Solar Energy Engineering*, no. 3, 2009.
13. D. Abel, *Regelungstechnik,* 35th ed.: Verlagsgruppe Mainz GmbH Aachen, 2011.
14. L. Oberkirsch, D. Maldonado Quinto, P. Schwarzbözl, and B. Hoffschmidt, *Solar Energy,* pp. 1089–1098, 2021
15. A. Zolan, W. Hamilton, K. Liaqat, and M. Wagner, HALOS (Heliostat Aimpoint and Layout Optimization Software): National Renewable Energy Laboratory (NREL), 2021.
16. R. Flesch, C. Frantz, D. Maldonado Quinto, and P. Schwarzbözl, *Solar Energy*, pp. 1273–1281, 2017.